Investigation of Reynold analogy of turbulent pipe flows with high *Pr*

Dong-Hyuk Park, Sang-Soo Yoon and Bum-Jin Chung*
Department of Nuclear Engineering, Kyung Hee University
#1732 Deogyeong-daero, Giheung-gu Yongin-si Gyeonggi-do 17104 Korea
**Corresponding author: bjchung@khu.ac.kr*

1. Introduction

Turbulent is widely used in engineering applications due to high heat transfer, including nuclear power plants. The friction also increases with the heat transfer in the turbulent flows, accompanying the pressure drop and pumping power increase parallel to the heat transfer depending on the flow configuration (geometry, flow rate, fluid properties). Therefore, an understanding of the relationship between heat and momentum transfers in the turbulent flow may help the system design.

The heat and moment equations for the fully developed turbulent flow are

$$u\frac{\partial u}{\partial x}+v\frac{\partial u}{\partial y}=\frac{\partial u}{\partial y}\left[(\nu+\varepsilon_m)\frac{\partial u}{\partial y}\right] \tag{1}$$

$$u\frac{\partial T}{\partial x}+v\frac{\partial T}{\partial y}=\frac{\partial T}{\partial y}\left[(\alpha+\varepsilon_h)\frac{\partial T}{\partial y}\right] \tag{2}$$

where ε_m and ε_h are the eddy momentum and thermal diffusivity respectively, which denote the influence of turbulence (eddy motion). By the definition of *Pr* and turbulent *Pr* ($Pr_t = \varepsilon_m / \varepsilon_h$), The Eq. (2) can be rewritten as below.

$$u\frac{\partial T}{\partial x}+v\frac{\partial T}{\partial y}=\frac{\partial T}{\partial y}\left[(\frac{\nu}{Pr}+\frac{\varepsilon_m}{Pr_t})\frac{\partial T}{\partial y}\right] \tag{3}$$

Comparing the Eq. (1) and (3), the difference of heat and momentum transfer in turbulent flow comes from the *Pr* and Pr_t. When these two terms are unity, the Eq. (1) and (3) is same and the heat and momentum transfer is same. This means that when we analyze the variation of *Pr* and Pr_t according to the flow configuration, it is possible to predict heat transfer through fluid friction (or fluid friction through heat transfer).

Reynolds (1900) proposed the direct relationship between shear stress and heat flux in turbulent flow with the assumption that the *Pr* and Pr_t are unity [1].

$$St = f/2 \tag{4}$$

After that, several authors extended the Reynolds analogy. Taylor (1916) and Prandtl (1928) considered the viscous sublayer in Reynolds analogy [1].

$$St=\frac{f/2}{1+5\sqrt{(f/2)}(Pr-1)} \tag{5}$$

In addition, von Karman (1939) considered the buffer layer [2].

$$St=\frac{f/2}{1+5\sqrt{(f/2)}\left\{Pr-1+\ln\left[(1+5Pr)/6\right]\right\}} \tag{6}$$

Colburn (1964) only multiplied the $Pr^{2/3}$ as a correction term in the Reynolds analogy [3]. The correction term was obtained from the existing simple geometry (plate and pipe) heat transfer and friction data with the *Pr* range 0.6-60.

$$St=(f/2)Pr^{-2/3} \tag{7}$$

Several studies have been conducted to validate the heat and momentum transfer analogies in low and medium *Pr* ranges. However, studies on high *Pr* fluid are scarce. In this study, we investigated the heat and momentum transfer analogies in high *Pr* using the copper sulfate-sulfuric acid ($CuSO_4$-H_2SO_4) electroplating system based on the analogy between heat and mass transfer. The *Sc* corresponding to the *Pr* is 2014. The pressure drop was measured spontaneously to compare with the heat transfer. A scale analysis was performed to obtain the relationship between heat and momentum transfer in high *Pr*.

2. Experimental setup and test matrix

2.1 Experimental methodology

Heat and mass transfer systems have analogous relationships, since their governing equations are mathematically the same. Thus, by using the mass transfer experiments, the heat transfer problems can be solved effectively.

The mass transfer coefficient (h_m) which corresponds to the heat transfer coefficient was calculated using the limiting current technique with a $CuSO_4$–H_2SO_4 electroplating system.

$$h_m=\frac{(1-t_{cu^{2+}})I_{\lim}}{nFC_b} \tag{8}$$

This technique has been developed by several researchers and is well-established as an experimental methodology [4,5].

2.2 Test matrix

Table 1 shows the test matrix of the present study. The *Sc* (*Pr*) was 2,014, which was determined by the concentrations of $CuSO_4$ (0.05 M) and H_2SO_4 (1.5 M). The pipe diameter (*D*) and length (*L*) are 0.02 m and 0.4 m respectively. The *L* is 20 *D* which the entrance effect can be neglected. The range of Re_D is 4,641-64,973 which corresponds to the turbulent flow regime.

Table I: Test matrix of present study

Sc (*Pr*)	*D* (m)	*L* (m)	Re_D
2014	0.02	0.4	4,641-64,973

2.3 Test Apparatus

Figure 1 shows the schematic diagram of the forced convection loop. The length of the flow path from the bending part to the test section is 50 *D*. Therefore, the flow was fully developed before entering the test section. The flow rate was controlled using a bypass valve and control valve. The electric current and pressure drop were measured using the data acquisition DAQ system.

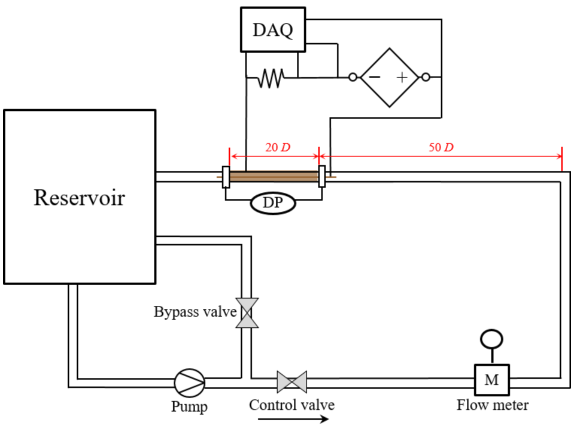

Fig. 1. Schematic diagram of forced convection loop.

3. Results and discussion

3.1 Reynolds analogy in high Pr

Before analyzing the Reynolds analogy at high *Pr*, an understanding of the relationship between *f*/2 and *St* is needed. The *f*/2 and *St* in turbulent flow are calculated as below

$$f/2 = \frac{\tau}{\rho u_b^2} \tag{9}$$

$$St = \frac{q''}{\rho u_b c_p (T_W - T_b)} \tag{10}$$

It is seen that *f*/2 is the ratio of the shear stress τ across the stream and momentum transfer per unit cross section with velocity u_b. Similarly, the *St* is the ratio of the heat flux q'' across the stream and heat carried per unit cross section with velocity u_b and temperature T_w-T_b. Thus, the meanings of *f*/2 and *St* are analogous.

Figure 2 shows the variation of (*f*/2)/*St* according to the Re_D. According to the Reynolds analogy, the ratio should be unity. However, the ratios are higher than 100. Reynolds analogy was developed for *Pr* =1, which means that only the turbulent core region was considered except for the viscous sublayer and buffer layer. However, in our case (*Pr* = 2014) the total thermal boundary layer thickness is smaller than the momentum viscous sublayer. Therefore, since the influence of turbulence (eddy motion) on heat transfer is smaller than momentum transfer, *St* is much smaller than *f*/2.

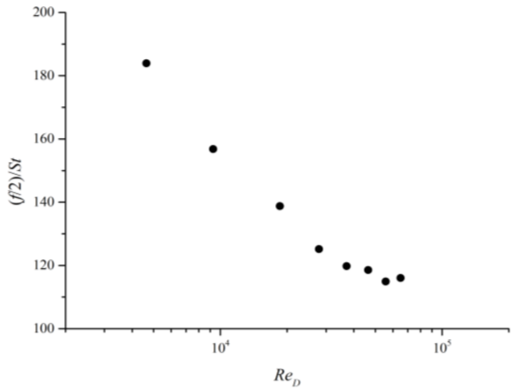

Fig. 2. Variation of (*f*/2)/*St* according to the Re_D.

3.2 Extended Reynolds analogy in high Pr

In this section, the *St* was calculated using the extended Reynolds analogies (Talor and Prandtl analogy [Eq. (5)], von Karman analogy [Eq. (6)] and Colburn analogy [Eq. (7)]) and compared with measured *St*. Fig. 3 compares the calculated *St* (St_c) and measured *St* (St_m) according to the Re_D.

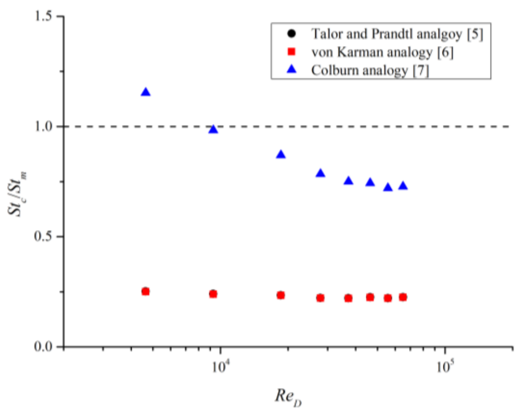

Fig. 3. Comparison of St_c and St_m according to the *Re*.

Taylor and Prandtl analogy and von Karman analogy have nearly the same values. The difference between the two analogies is whether the buffer layer influence is considered. Due to the thin thermal boundary layer in high *Pr*, the influence of the buffer layer hardly appeared. The St_c is nearly five times smaller than St_m. The *Pr* term in Eq. (5) represents the ratio of momentum diffusivity and thermal diffusivity in viscous sublayer. If the thickness of the momentum viscous sublayer and thermal viscous (conduction) sublayer are in the same order, the momentum and thermal eddy diffusivity (ε_m and ε_h) can be excluded. However, since the conduction sublayer is much smaller than the viscous sublayer in the high *Pr*, the ε_h cannot be excluded in the viscous sublayer. Therefore, in high *Pr* case, the effective *Pr* in Eq. (5) should be $\nu/(\alpha+\varepsilon_h)$ rather than ν/α. This means that the Prandtl and Taylor analogy overestimate the *Pr* influence in High *Pr*.

The Colburn analogy predicted well the measured *St* with among these analogies. However, the difference according to the Re_D is quite large. This means that the Colburn analogy could reduce the difference due to *Pr*, but the difference due to *Re* could not be reduced.

3.3 Development of St and f/2 correlation in high Pr

To develop the correlation between *St* and *f*/2 applicable in high *Pr*, scale analysis was performed.

In viscous sublayer ε_m can be ignored compared to the ν but ε_h cannot be ignored due to the small thickness of the conduction sublayer. Therefore, the shear stress and heat flux in viscous sublayer can be written as follows.

$$\tau = \rho\nu\frac{\partial u}{\partial y} = \rho\nu\frac{u_{vsl}}{\delta_{vsl}} \tag{11}$$

$$q'' = -\rho c_p(\alpha+\varepsilon_h)\frac{\partial T}{\partial y} = \rho(\alpha+\varepsilon_h)\frac{T_{vsl}-T_w}{\delta_{vsl}} \tag{12}$$

Using the Eq. (11) and Eq. (12), the below equation can be obtained.

$$\frac{1}{1/Pr+\nu/\varepsilon_h}u_{vsl}\frac{q''}{\tau} = c_p(T_{vsl}-T_w) \tag{13}$$

In the turbulent core regime, ν and α can be excluded compared to ε_m and ε_h. Therefore, the shear stress and heat flux in turbulent core regime can be written as below.

$$\tau = \rho\varepsilon_m\frac{\partial u}{\partial y} = \rho\varepsilon_m\frac{u_b-u_{vsl}}{\delta_b} \tag{14}$$

$$q'' = -\rho c_p\varepsilon_h\frac{\partial T}{\partial y} = \rho c_p\varepsilon_h\frac{T_b-T_{vsl}}{\delta_b} \tag{15}$$

Using the Eq. (14) and Eq. (15), the below equation can be obtained.

$$Pr_t(u_b-u_{vsl})\frac{q''}{\tau} = c_p(T_b-T_{vsl}) \tag{16}$$

Combining Eq. (13) and (16) and by the definition of q'' and τ the below relationship can be obtained.

$$\frac{h}{\rho u_b c_p} = St = \frac{f/2}{Pr_t+(\beta-Pr_t)u_{vsl}/u_b} \tag{17}$$

$$\beta = \int_0^{y_{vsl}}\frac{1}{1/Pr+\nu/\varepsilon_h}dy \tag{18}$$

To solve the Eq. (17), the information about u_{vsl}/u_b and β is needed. In viscous sublayer, the below relationship was revealed [6].

$$u^+ = y^+ \tag{19}$$

$$\varepsilon_h/\nu \sim y^{+1/3} \tag{20}$$

Where y^+ and u^+ are non-dimensional wall coordinate which are calculated as $y(\tau/\rho)^{1/2}/\nu$ and $u/(\tau/\rho)^{1/2}$ respectively. At viscous sublayer, y^+ is nearly 5, thus u_{vsl}/u_b and β can be calculated as below.

$$\frac{u_{vsl}}{u_b} = 5\sqrt{\frac{\tau}{\rho u_b^2}} = 5\sqrt{\frac{f}{2}} \tag{21}$$

$$\beta = \int_0^5\frac{1}{1/Pr+\nu/\varepsilon_h}dy^+ \sim Pr^{-1/3} \tag{22}$$

Assuming the Pr_t is 1 and substituting the Eq. (21) and (22) into Eq. (17), the *St* can be calculated as followed.

$$St = a\frac{f/2}{1_t+5\sqrt{(f/2)}(Pr-1)Pr^{-1/3}} \tag{23}$$

Where a is constant. In High *Pr*, Eq. (23) can be simplified in the below form.

$$St = a\left(f/2\right)^{1/2}Pr^{-2/3} \tag{24}$$

The *a* is 0.682 which calculated using the experimental data in this study. Fig. 4 shows the compared St_m and St_c calculated by Eq. (24). The Eq. (24) predicted well the *St* compared to the existing extended Reynolds analogy in Fig. 3.

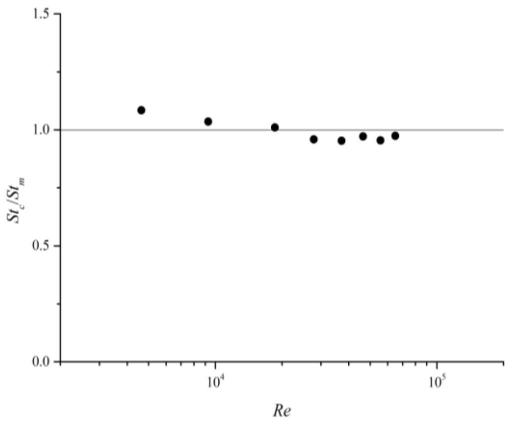

Fig. 4. Variation of St_c/ St_m according to the Re_D by Eq. (24).

4. Conclusions

The mass (heat) transfer rate and pressure flow were measured simultaneously to investigate the relationship between heat and momentum transfers. The $CuSO_4$–H_2SO_4 electroplating system was adopted to obtain high *Pr*. The measured heat and momentum data were compared using the existing analogy equations.

According to the Reynolds analogy, the $f/2$ should be the same with the *St*. However, the $f/2$ is nearly 100 times higher than *St* at Pr =2014. Since the thermal boundary layer is thinner than viscous sublayer, the influence of turbulence on heat transfer is much weaker than momentum transfer.

Among the extended Reynolds analogies, Coburn predicted well measured *St*, but the difference according to the *Re* was appeared. The calculated *St* using Taylor and Prandtl analogy and von Karman analogy are five times lower than the measured value since both analogies overestimate the *Pr* influence in high *Pr* fluid.

A correlation between *St* and $f/2$ for high *Pr* was developed using the scale analysis. The developed correlation well predicted the measured *St* compared to the existing extended Reynolds analogy within 10 % error.

ACKNOWLEDGEMENT

This study was sponsored by the Ministry of Science and ICT (MIST) and was supported by nuclear Research & Development program grant funded by the National Research Foundation (NRF) (Grant codes 2020M2D2A1A02065563)

REFERENCES

[1] A. Bejan, Convective heat transfer, John Wiley & Sons, New York, pp.310-361, 2013.
[2] T. von Karman, “The Analogy Between Fluid Friction and Heat Transfer”, Transactions of the American Society of Mechanical Engineering, Vol. 61, p.705-710, 1939.
[3] A. P. Colburn, “A method of correlating forced convection heat-transfer data and a comparison with fluid friction”, International Journal of Heat and Mass Transfer, Vol. 7, pp. 1359-1384, 1964.
[4] J.R. Selman and C.W. Tobias, Mass-transfer measurement by the limiting-current technique, Advance in Chemical Engineering, Vol 10, p. 211-318, 1978.
[5] C.W. Tobias and R.G. Hickman, Ionic mass transport by combined free and forced convection, International Journal of Research in Physical Chemistry Chemical Physics, Vol. 229, p. 145-166, 1965.
[6] R.H. Notter and C. A. Sleicher, “The eddy diffusivity in the turbulent boundary layer near a wall”, Chemical Engineering Science, Vol. 26, pp. 161-171,1971.